

# Fabrication of Nanoscale Plasmonic Structures and Their Applications to Photonic Devices and Biosensors

Woo Kyung Jung and Kyung Min Byun

Received: 5 August 2011 / Accepted: 8 August 2011

© The Korean Society of Medical & Biological Engineering and Springer 2011

## Abstract

In this review, we explored the fabrication and application of various metallic nanostructures that support localized surface plasmons. Principles and unique characteristics for individual nanopatterning technologies were demonstrated and relevant discussion focused on the process cost, throughput, and possibilities of large-area patterning and mass production. As a potential use of the nanoscale plasmonic structures, several applications such as plasmonic light sources, photovoltaic devices, and localized surface plasmon resonance biosensors were investigated. In conclusion, true realization of such promising applications could be accomplished through an advance in nanofabrication techniques, together with a better understanding of the underlying fundamentals and a greater collaboration in a variety of fields.

**Keywords** Surface plasmon, Localized surface plasmon, Nanofabrication, Lithography, Metallic nanostructure, Nanoimprint, Photonic device, Biosensor

## INTRODUCTION

Surface plasmons (SPs) are propagating waves of longitudinal electron oscillations at the interface between a metal and a dielectric, which are coupled to a light field [1]. When a momentum matching between a SP and an incidence beam occurs, the field intensity of SP waves reaches a maximum at the interface and decays exponentially in the perpendicular directions. The propagating distance of SP waves is restricted in the horizontal plane by an absorption property of the metal film [2, 3]. Due to this field confinement, it has steadily

evolved towards the use of surface plasmon-based photonics, or plasmonics, for manipulating light at the nanoscale. The promising research field of plasmonics is not only aimed at developing miniaturized optical devices and integrated photonic circuits. Since the resonance condition of SP waves are very sensitive to the presence of slight perturbations in refractive index within the penetration depth, SPs are of interest to a wide community of researchers in the area of an optical biosensor [4]. Moreover, surface plasmon resonance (SPR) technique has attracted much attention through a recent advance in nanofabrication methodologies and has extended its potential applications to microscopic imaging, lithography, light sources, and energy conversion [5]. Involving these exciting opportunities, a variety of approaches have been made to answer the question of how the plasmon excitation can be used advantageously, in order to overcome the limitations of traditional photonic devices.

In contrast to propagating SP waves, metallic nanoparticles allow a direct and strong optical coupling of the incident light to resonantly driven electron charge oscillations, called localized surface plasmons (LSPs) [6]. The LSP resonance (LSPR) excitation induces substantial enhancement of electromagnetic fields as a result of strong absorption and light scattering. The spectral position and magnitude of the LSPR depends on the material, size, and shape of the nanoparticles, as well as on the surrounding local medium [7-9]. Although the SP waves provoked by a planar metal surface show a relatively large penetration depth of several hundred nanometers, it is interesting to note that the penetration depth of the LSP mode associated with metallic nanoparticles can be considerably smaller, of order 10 nm [10], owing to the divergence of the electric field around the sharp edges of such structures [11]. Interestingly, this localization of the field near the metallic surface is accompanied by an enhancement of the field intensity, which is attributed to the associated increase in the local photonic mode density [12]. Tight field confinement to the nanoparticle

Woo Kyung Jung, Kyung Min Byun (✉)  
Department of Biomedical Engineering, Kyung Hee University, Yongin  
446-701, Korea  
Tel : +82-31-201-3842 / Fax : +82-31-202-1723  
E-mail : kmbyun@khu.ac.kr

surface and giant field amplification make the LSP mode very sensitive to surface irregularities, so that LSPs have been intensively used in surface analysis [4, 13].

Another possible approach for expanding the range of available LSP mode is to induce an interaction between two or more nanoparticles separated by very small distances. Within the decay length of the LSP modes, electromagnetic coupling of individual nanostructures has a prominent influence on the resonance condition and consequently, the interaction between the neighboring nanoparticles can lead to a new hybridized plasmon mode, called hot-spot [14, 15]. This interparticle plasmon coupling forms the basis of the intense enhancement of spectroscopic signals, for example, surface-enhanced Raman scattering (SERS), from molecules adsorbed at the nanoparticle gaps, providing the capability for single molecule detection [16]. Besides, near-field coupling in ordered nanoparticle assemblies has been exploited for electromagnetic energy transport and subwavelength photonic waveguiding [5].

Field enhancement by plasmonic coupling effects essentially requires an integration of dense arrays of metallic nanoparticles with control over dimension tolerances at the nanometer scale. One general approach for achieving locally enhanced fields is to use aggregated colloidal metallic nanoparticles. However, owing to the stochastic nature of the nanoparticle aggregates, resonant LSP mode has a relatively low probability of occurring by random aggregation [17]. Hence, various plasmonic structures for reproducibly enhancing the electromagnetic fields have been explored. Recently, rapid advances in nanofabrication open up the possibility of manipulating the optical properties in a controllable way and tailoring them for specific applications.

In this review, we will overview various plasmonic nanostructures fabricated with the use of well-established lithography approaches since recent innovations of the lithographic processes provide a powerful means to explore a wide range of structures with an excellent control. Next, we focus on the formation of LSP modes and their applications to a variety of photonic devices, including plasmonic light sources, photovoltaic devices, and LSPR-based biosensors. Finally, several concluding remarks will be provided.

## FABRICATION OF PLASMONIC NANOSTRUCTURES

### Direct-write lithography

Lithography is the process of transferring patterns from one substrate to another. For recent years, particle beams of various types have been used in lithography. The direct-write systems use a finely focused Gaussian particle beam that moves with the wafer to expose one pixel at a time. When

one should deal with subwavelength periodicities and feature sizes of the order of 100 nm, such feature sizes are smaller than the resolution of state-of-art photolithography and nanofabrication process with sub-100 nm resolution is thus highly required. Electron-beam lithography (EBL) is one of the most widely used particle beam techniques, which can produce arbitrarily shaped particles of good features and various sizes. EBL also offers good reproducibility and high spatial resolution, approximately down to 10 nm [18].

EBL technique is generally combined with the lift-off process to add desired materials to the substrate. In an actual EBL process, the electron-beam resist coating is exposed by electron-beam and the exposed resist is developed and removed in a solvent. The patterned resist is then used as a sacrificial mask in subsequent etching or deposition processes to generate metallic nanostructures. The final step of the lift-off process is accompanied by soaking the substrate in a solvent bath to wash away both the remaining resist and the unwanted materials [19]. As listed in Table 1, the plasmonic structures ranging from 1D subwavelength gold nanogratings for selective immobilization of functional surface ligands to 2D metallic nanorings, pyramids, and nanocylinders for sensitive biosensing have been fabricated using EBL techniques [20-27].

Focused ion beam (FIB) lithography is another important scanning beam technique. FIB milling has been the most common method to fabricate arrays of hole and slot structures in optically thick metal films [28]. This method has been often utilized to investigate the extraordinary optical transmission (EOT) phenomenon [28, 29]. From the experiments on the light transmission through arrays of nanoholes in thin gold and silver films, the discovery of enhanced optical transmission at certain wavelengths exceeded the amount predicted by the classical aperture theory and revealed that the wavelength of the maximum transmission could be dependent on the size, period, and geometry of the nanoholes. While plasmonic interpretation on the EOT is still underway, the resonant excitation of SP waves seems to play an important role in this enhanced transmission. Specifically, light incident to the nanohole arrays excites SP waves on one side of the metallic film, which tunnel through the holes and increase the efficiency of light transmitted through the holes. Then, the SP waves generated at the opposite side of the film scatter from the nanohole array and are finally converted into an emitted light [30, 31].

For accurate nanohole fabrication, the ion beam path and irradiation interval should be designed in advance because the high-intensity ion beam with a Gaussian distribution may cause a redeposition of sputtered material, decreasing the accuracy of the machining [32]. Proper process scheduling for FIB milling allows the diameter and spacing of the

**Table 1.** Nanoscale plasmonic structures based on EBL technique.

Plasmonic nanostructure	Geometric parameters	Pattern size	Application
2D Au and Ag nanocylinders	D = 100 nm T = 50 nm $\Lambda$ = 200 nm	$80 \times 80 \mu\text{m}^2$	11-MUA, PDDA, and PSS sensing [20]
1D Au nanogratings	W = 200 nm T = 40 nm $\Lambda$ = 400 nm	$250 \times 250 \mu\text{m}^2$	Guided immobilization of functional surface receptors [21]
2D double slit Au and Ag nanorings	R = 150 & 200 nm T = 20 nm $\Lambda$ = 500 nm	Not provided	Enhanced Raman sensing [22]
2D Au nanodots	D = 70 ~ 550 nm T = 20 nm $\Lambda_x$ = 300 ~ 600 nm $\Lambda_y$ = 300 nm	$100 \times 100 \mu\text{m}^2$ ~ $400 \times 400 \mu\text{m}^2$	Photonic crystal structure for low-loss wave propagation and small damping [23]
2D Au nanopyramids	T = 70 nm $\Lambda$ = 200 nm	$40 \times 40 \mu\text{m}^2$	Raman sensing of R6G molecules [24]
Connected or disconnected 2D Au nanotriangles	S = 100 nm G = 25 nm T = 15 nm $\Lambda > 500$ nm	$70 \times 70 \mu\text{m}^2$	High-resolution mapping of LSP modes [25]
Pair of 2D Au nanoblocks	S = 100 nm G = 5 nm T = 40 nm $\Lambda$ = 500 nm	$30 \times 30 \mu\text{m}^2$	Photopolymerization of TiO <sub>2</sub> -organic hybrid materials [26]
2D Au nanorods	W = 55 nm L = 385 nm T = 32 nm $\Lambda_x$ = 400 nm $\Lambda_y > 500$ nm	$30 \times 30 \mu\text{m}^2$	Selective photopolymerization of SU-8 [27]

D: diameter,  $\Lambda$ : period, T: thickness, W: width, R: radius, S: side, G: gap, L: length

nanostructures to have a reasonable precision less than 100 nm. Recently, various metallic nanostructures such as random and periodic nanohole arrays, slit gratings, tapered slits have been fabricated by FIB [33]. Fig. 1 shows the 1D periodic arrays of tapered slits fabricated using FIB milling in a 180 nm-thick gold film [34]. The experimentally investigated structures had a fixed taper angle of 20.5° for two different widths of 80 and 130 nm, having gaps of 25 and 65 nm, respectively, fabricated at two different periods,  $\Lambda = 500$  and 700 nm. Using well-established two-photon photoluminescence (PL) experiment for the evaluation of the transmitted field enhancement, the obtained enhancement reached 110 times for the slits of  $\Lambda = 500$  nm and a gap size = 25 nm. This enormous enhancement is attributable to the nanofocusing and the resonant interference of counter-propagating plasmons by the tapered gaps.

It should be also noted that plasmonic arrays consisting of metallic nanoparticles or subwavelength holes in a metal film be patterned on a large area for a wider range of practical applications. However, due to the low throughput of serial point-by-point direct-write and its high fabrication cost, only small patterned areas can be obtained. Thus, development of high precision and high throughput manufacturing process

is required and the relevant examples of such techniques are nanosphere lithography (NSL), laser interference lithography (LIL), and nanoimprint lithography (NIL).

### Nanosphere lithography

NSL is less expensive and more parallel method which utilizes a colloidal crystal mask based on a self-assembly technique [33]. Recent progress in NSL has shown that this method provides a good template for shape-controlled fabrication of surface-confined nanoparticles [35]. Van Duyn and co-workers used a hexagonal close-packed monolayer nanosphere on a substrate as a mask of deposition or etching to generate metal nanoparticles arrays [36]. In general, NSL process begins with the deposition of a single-layer colloidal crystal mask which contains triangular nanovoid structures between neighboring particles. In subsequent deposition processes, metal is deposited through the mask and finally, by removing the nanosphere templates, hexagonally arranged triangular nanoparticles can be obtained. The routine NSL process involving the colloidal nanosphere mask and the metallic nanoparticle arrays is shown in Fig. 2 [35, 37].

As advanced structures, if triangular nanoparticles are sonicated to remove a weak tip, annealed for several hours,

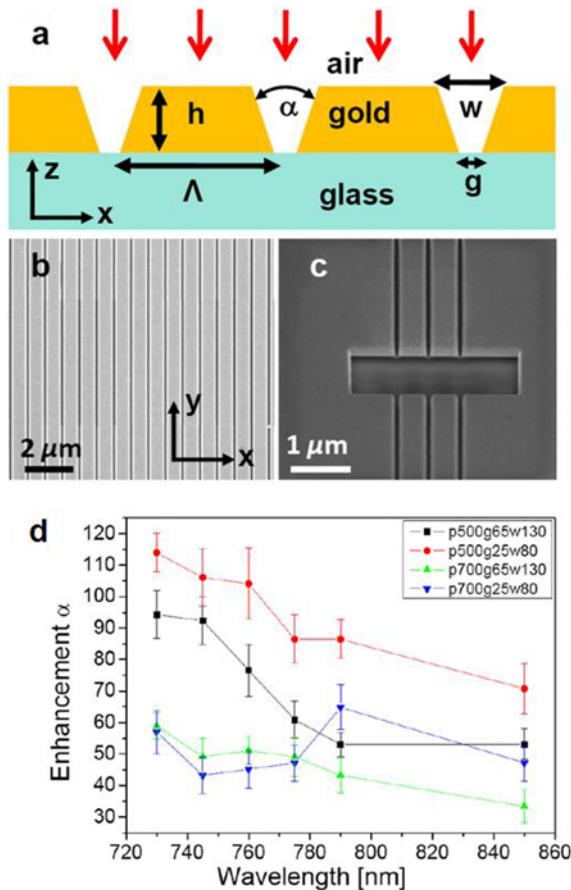


**Fig. 1.** (a) Schematic of 1D periodic line arrays of parallel tapered slits in a 180-nm thick gold film, with each array covering  $30 \times 30 \mu\text{m}^2$  and separated from other arrays by at least  $500 \mu\text{m}$ . The taper angle is fixed at  $\alpha = 20.5^\circ$ . (b) SEM image of the array with slit top width  $w = 80 \text{ nm}$ , bottom gap  $g = 25 \text{ nm}$ , and period  $\Lambda = 700 \text{ nm}$  and (c) zoomed SEM image of a tilted test array with  $w = 80 \text{ nm}$ ,  $g = 25 \text{ nm}$ , and period  $\Lambda = 500 \text{ nm}$ . (d) Experimental dependence of the intensity enhancement from the slit arrays on an excitation wavelength ranging from 730 to 850 nm obtained for p-polarization. (Reprinted with permission from [34]. Copyright 2011 IOP Publishing Ltd.)

and washed with nitric acid sequentially, metallic nanoparticles with rounded edges can be formed. Moreover, we may tune the optical properties of the metallic nanoparticles through an introduction of  $\text{O}_2$  reactive ion etching process to control the diameter of the nanospheres precisely, which is attributed to the fact that the nanosphere diameters could be continuously reduced by increasing the etching time with a high linearity [35]. As a result, the size and shape of the nanoparticles can be changed in a controllable way and NSL allows low-cost, versatility, and capability to manufacture the sub-100 nm array structures.

### Laser interference lithography

LIL is a maskless lithographic technique, which makes use of the interference pattern of two incident laser beams and

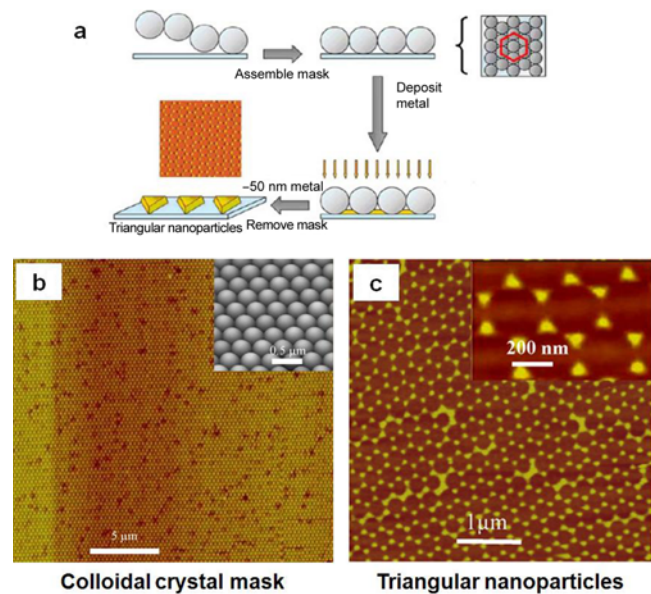


**Fig. 2.** (a) Nanosphere lithographic fabrication of triangular nanoparticles in the interstices between the elements of the nanosphere deposition mask, (b) nanosphere templates based on 290 nm spherical polystyrene nanospheres for Ag nanoparticle fabrication, and (c) AFM image of an area of surface-confined triangular prism Ag nanoparticles. The inserted magnified image shows the weak tips and rough surface morphologies. (Reprinted with permission from [35, 37]. Copyright 2005 & 2010 Elsevier.)

records the pattern on a photoresist material. While the EBL method suffers from the costly instrumentation, low throughput rate, and small patterned areas and the NSL method is suitable only for arrays with hexagonal symmetry [38], LIL has proven its ability to generate uniform 2D patterns over a large area. LIL requires only simple experimental setups, and more importantly, various structures are feasible by tuning the beam orientation, interference angle, and polarization. Furthermore, it allows mass production of particle arrays in large and uniform areas at a much lower cost compared to the EBL method [38, 39].

LIL can be simply performed using Lloyd's configuration [40]. The Lloyd holder is attached on a rotating stage with a high angle precision to have a fine control of the periodicity. The laser light should have a long coherence length, sufficient to prevent phase changes after the beam expands from the spatial filter. The spatial filter allows high frequency noise to be removed from the beam [41]. Interference between the light coming directly from the spatial filter and its mirror image forms a standing wave pattern on the substrate. The interference pattern has a sinusoidal profile whose intensity varies with a period equal to  $\Lambda = \lambda / (2 \sin \theta)$ , where  $\lambda$  is the wavelength of the laser beams, and  $\theta$  is the half angle at which two beams intersect. From the above relation of the grating constant  $\Lambda$ , the minimum feature size is approximately equal to  $\lambda/2$  and thus, sub-100 nm resolution is not achievable

by the light source in the visible band. To overcome this limitation on the feature size, recent LIL techniques are often combined with ultraviolet (UV) or extreme ultraviolet (EUV) sources [42]. Practically, however, the change of the illumination wavelength to shorter one implies new light sources, optics, and photoresists that become more complex with a decreasing wavelength. Also, one may suffer from the low energy electrons released by EUV and additional adverse effects such as photopolymer aggregates, shot noise, and proximity effect, which could blur the original EUV pattern.

### Nanoimprint lithography

Unlike the above lithographic techniques, where nanoscale patterns are defined by the modification of the chemical and physical properties of the resist, NIL is based on the direct mechanical deformation of the resist. Thus, the resolution achievable with NIL is beyond the limitations caused by light diffraction or beam scattering in other optical lithographies [43].

Conventional NIL uses solid-phase thermoplastic polymers such as polymethylmethacrylate (PMMA) as an imprint resin, due to its ability to form high-resolution patterns [44]. PMMA resin requires a high imprint temperature larger than 170°C and an imprint pressure as high as 50 bar in order to transfer nanoscale patterns defined at a stamp mold into the PMMA layer. In Fig. 3, pressing the stamp yields a thickness contrast in the imprint resin and a few tens of nanometer thick residual layer remains inevitably after imprinting, which is attributed to limited fluidity of PMMA resin. After

the separation process, the residual layer can easily be removed by oxygen plasma etching [43]. However, lateral dimension and profile of the imprinted resin can be somewhat degraded during this step. Another NIL approach, called UV nanoimprint lithography uses UV curable liquid-phase imprint resin. Since liquid-phase imprint resin can be solidified by UV exposure, imprinting can be done at room temperature and imprint pressure can be lowered drastically [45]. Since UV light is used to polymerize the resin, either substrate or imprint template must be transparent to UV light.

As emphasized previously, the lithographic technique suitable for practical applications should offer the simplicity of usage and the possibility of adapting the procedure for various designs. NIL is one such technique that provides high precision, mass production, reproducibility, and large-scale integration of the plasmonic structures. In particular, NIL-based fabrication can be extended into more complex structures, including plasmonic waveguides for the optical interconnection and communication and the microfluidic channels for chemical biosensing and lab-on-a-chip devices [46]. This makes NIL considered as the most promising next generation nanopatterning technique.

## APPLICATION TO PHOTONIC DEVICES AND BIOSENSORS

### Plasmonic light source

The fabricated plasmonic structures can help to improve the extraction efficiency of light emitting diodes (LEDs) through an increase of the spontaneous recombination rate of the emitters. This approach is based on the energy transfer between light emitters and SP waves [5]. For example, Okamoto *et al.* demonstrated a significant enhancement of the internal quantum efficiency of semiconductor quantum wells by controlling the energy transfer between quantum wells and plasmon waves [47, 48]. Another approach for enhancing the light emission from the active layer is to use a photonic crystal structure by slowing the propagation speed of the photons and thus increasing the coupling to the out-of-plane radiative modes. Reboud *et al.* utilized the NIL technique to combine the both effects of a surface plasmon and a photonic crystal on the light-emission efficiency and reported a 27-fold enhancement of PL intensity at room temperature by fabricating a photonic crystal with dyes in the vicinity of a silver film [49]. This enhancement is attributed to the light coupling to the leaky modes of the photonic crystal slab structure and to the coupling of the emitted photons to surface plasmons. In recent years, Gwon *et al.* investigated the optical properties of ZnO/Ag grating structures fabricated by NIL. It was found that the grating

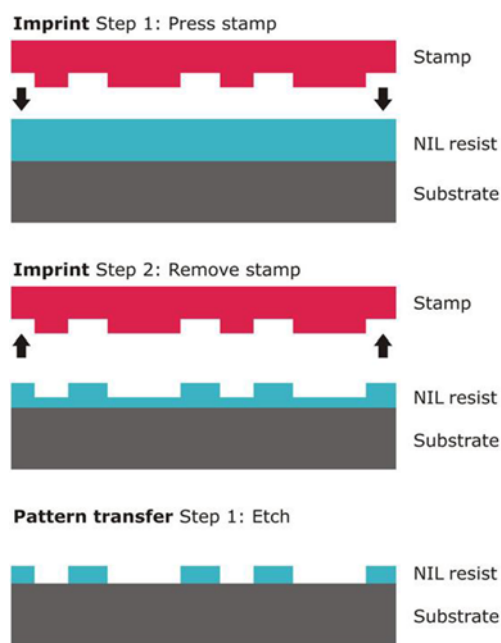


**Fig. 3.** Schematic of the originally proposed nanoimprint lithography process where a resist layer is used for pattern transfer. (Reprinted with permission from [43]. Copyright 2009 IOP Publishing Ltd.)

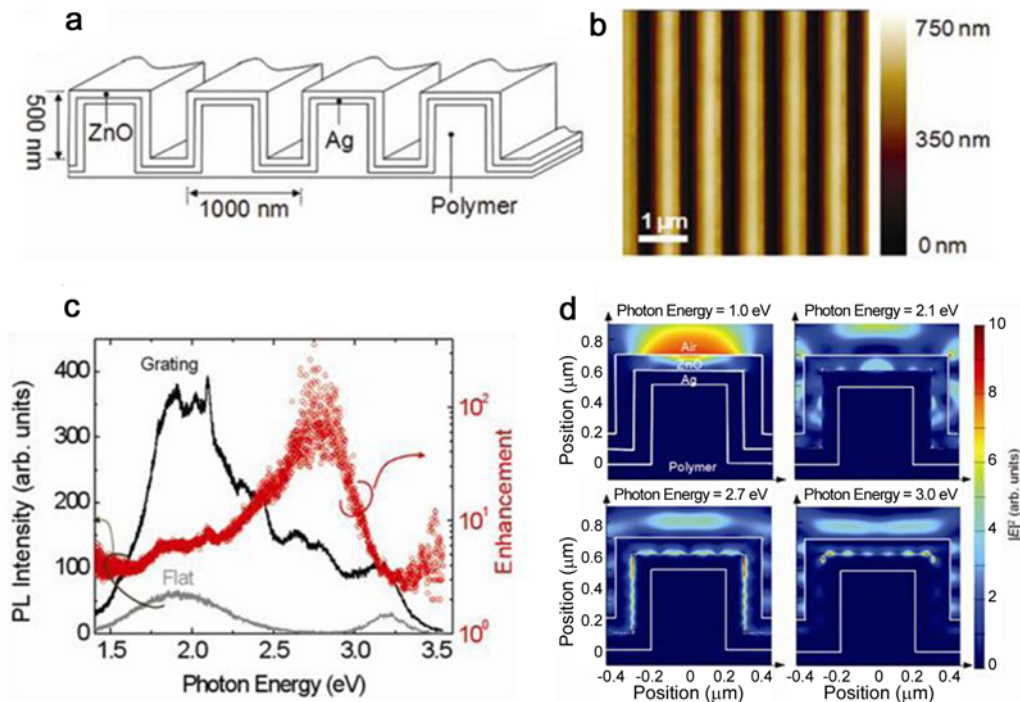


**Fig. 4.** (a) Schematic of a ZnO/Ag grating structure, (b) AFM morphology of a polymer pattern with a period of 1  $\mu\text{m}$  and a line-to-space ratio of 1:1, (c) PL spectra of a ZnO/Ag planar thin film and a ZnO/Ag grating structure. Enhancement indicates the ratio of the PL intensity of the grating structure to that of the planar thin film. (d) Electric field intensity distribution of a ZnO/Ag grating structure at various photon energies obtained by FDTD simulations for p-polarized plane waves. (Reprinted with permission from [50]. Copyright 2011 Optical Society of America.)

structures exhibited multiple peak features in broad visible-range PL spectra and the PL intensity of the grating was much larger than that of a planar thin film by up to two orders of magnitude (Fig. 4) [50]. These results also support that NIL technique is a well-suited process to fabricate the challenging photonic devices based on the plasmonic effects.

### Photovoltaic devices

Development of photovoltaic devices for efficient conversion

of sunlight to electricity is a promising research area of plasmonics [51]. Conventionally, photovoltaic absorbers must be optically thick to allow almost complete light absorption and photocarrier current collection. For thick Si solar cells, light-trapping is typically achieved using a pyramidal surface texture that causes scattering of light into the solar cell over a large angular range, therefore increasing the effective path length in the cell. Such large-scale geometries, however, are not suitable for thin-film cells. Also, the greater surface area

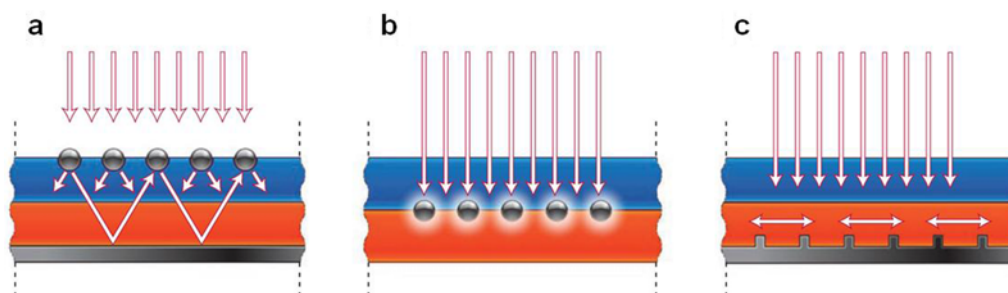


**Fig. 5.** Plasmonic light-trapping geometries for thin-film solar cells. (a) Light-trapping by scattering from metal nanoparticles at the surface of the solar cell. Light is preferentially scattered and trapped into the semiconductor thin film by multiple and high-angle scattering, causing an increase in the effective optical path length in the cell. (b) Light-trapping by the excitation of localized surface plasmons in metal nanoparticles embedded in the semiconductor. The excited particles' near-field causes the creation of electron-hole pairs in the semiconductor. (c) Light-trapping by the excitation of surface plasmon polaritons at the metal/semiconductor interface. A corrugated metal back surface couples light to SP waves or photonic modes that propagate in the plane of the semiconductor layer. (Reprinted with permission from [52]. Copyright 2010 Nature Publishing Group.)

increases minority carrier recombination in the surface and junction regions [52].

Alternative plasmonic approach to achieve light-trapping in thin-film solar cells is the use of metallic nanostructures. By engineering the plasmonic nanostructures, light can be concentrated and folded into a thin semiconductor layer, thereby increasing the absorption. As shown in Fig. 5, plasmonic structures can offer three possible ways of reducing the physical thickness of the photovoltaic absorber layers while keeping their absorption efficiency constant [52]. First, metallic nanoparticles can be used as subwavelength scattering elements to couple and trap freely propagating plane waves from the sunlight into an absorbing semiconductor thin film, by folding the light into a thin absorber layer. Second, metallic nanoparticles can be used as subwavelength antennas in which the enhanced local field is coupled to the semiconductor, increasing its effective absorption cross-section. Third, a corrugated metallic film on the back surface of a thin photovoltaic absorber layer can couple the sunlight into propagating plasmon modes supported at the metal/semiconductor interface as well as guided modes in the semiconductor slab, and the light is therefore converted into photocarriers in the semiconductor.

For highly efficient absorption property, the plasmonic substrate requires an integration of dense arrays of metal nanostructures over a large-area surface. In order to improve the fabrication cost, throughput, and reproducibility, a large-area photovoltaic module should be produced by inexpensive and scalable techniques for fabricating metallic nanostructures in a controlled way. Kang *et al.* demonstrated organic solar cells with transparent Ag nanowire electrodes using NIL method. The enhancement in quantum efficiency and short circuit current lead to an improved power conversion efficiency of the Ag device by about 35%, compared to that of the ITO device under unpolarized light illumination [53]. They also asserted that the photon to current efficiency can be enhanced by adjusting the period of the Ag nanograting such that SP enhanced spectral range matches the peak absorption of the organic semiconductors.

### LSPR biosensor

Since the peak wavelength and its magnitude of LSPR are sensitive to changes in the local environment caused by molecules adsorbed onto the nanostructures, LSPR devices can serve as a transmission-type biosensor [54]. Relative to a conventional SPR scheme, an optical setup to characterize an extinction-based LSPR biosensor is compact and potentially easier to use because it is based on wavelength scanning at normal incidence and allows the light source and the detector to be positioned on opposite sides. A more important characteristic of an LSPR biosensor is its capability for high-throughput monitoring, for example, in DNA research and

proteomics for which thousands of binding interactions should be examined rapidly [21, 55].

One of the important issues of current LSPR biosensor research is the sensitivity enhancement. The improved sensitivity based on the plasmonic nanostructure is associated with an increase of reaction area and, more critically, a strong interplay of target analytes with the excited LSP modes [56]. In other words, when a biomolecular interaction is exposed to highly localized fields, the resonance shift as a result of the biointeraction could be stronger. While the sensitivity may not be governed by only one factor, recent theoretical and experimental results have verified that this effect may be true [17, 57]. In the subsequent paragraph, we will briefly demonstrate how to make the most of the

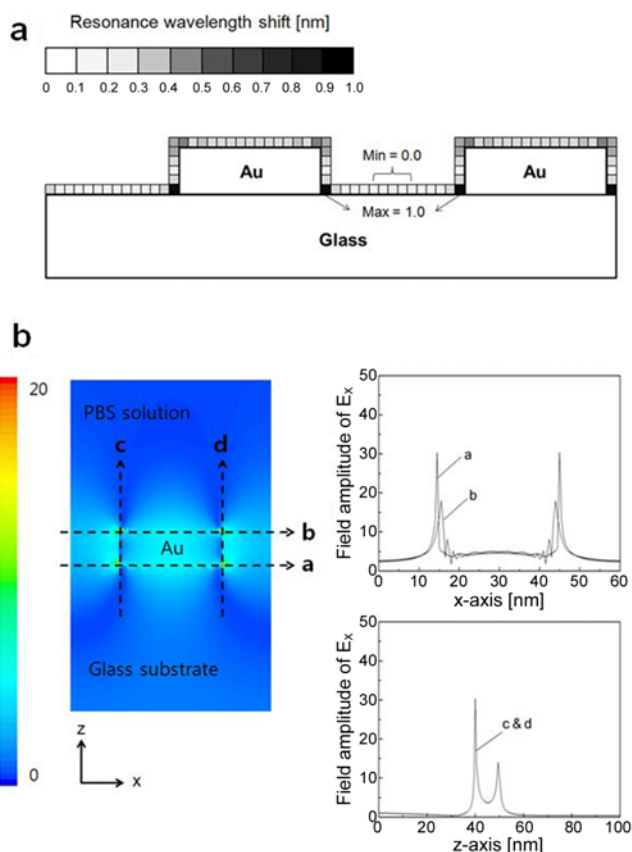


**Fig. 6.** (a) Resonance wavelength shift characteristics of the LSPR substrate with 10-nm thick gold nanogratings in PBS environments. The grating structure of a rectangular profile has a period of  $\Lambda = 60$  nm and a duty cycle = 0.5. TM-polarized white light source is normally incident to the gold nanogratings directly deposited on SF10 glass substrate. When a  $2 \text{ nm} \times 2 \text{ nm}$  dielectric element moves along the sensor surface and its refractive index increases from 1.40 to 1.60, the highest sensitivity is obtained to be 5.0 nm/RIU at the lower corners of a gold nanograting and the minimum sensitivity of 0.0 nm/RIU is found at the center areas between gold nanogratings. (b) Horizontal and vertical field distributions of  $E_x$  for the LSPR structure of (a). The 2D image obtained from the FDTD calculation is normalized by the field amplitude of 20.

nanostructured plasmonic substrates by coinciding the localized target molecules and the evanescent near fields. Instead of a simple use of metallic nanostructures, selective target localization in the locally enhanced fields could open up a possibility of maximizing the detection sensitivity.

Fig. 6 shows the numerical results for an LSPR structure with subwavelength gold nanogratings of a period = 60 nm, a thickness = 10 nm, and a duty cycle = 0.5 [58]. Using rigorous coupled-wave analysis, when a refractive index of  $2 \text{ nm} \times 2 \text{ nm}$  dielectric sample varies, the highest refractive index sensitivities are obtained to be 5.0 nm/RIU at the lower grating corners and the second sensitivity peaks of 2.5 nm/RIU are found near the upper grating corners. Hence, it is obvious that the binding events associated with the localization at the grating corners make a significant contribution to achieving a high sensitivity. In particular, no refractive index shift is found when the dielectric element is deposited on a glass substrate and is more than 10 nm apart from the gold gratings. From these results, we can suppose that the evanescent field produced at the analyte interface is responsible for this non-uniform distribution of the sensor sensitivity. To verify the correlation between the refractive index sensitivity and the local plasmon field, horizontal and vertical field amplitudes are calculated at a normal incidence. Finite-difference time-domain (FDTD) results show that the two main resonances are found on the lower corners of the nanograting and the secondary peaks on the two upper corners. In other words, the field distribution is exactly consistent with the sensitivity profile. On the assumption of an incident light of unit amplitude and a grid size of 0.5 nm, maximum field amplitudes are obtained as  $E_x = 30.3$ ,  $H_y = 4.0$ , and  $E_z = 23.2$ . While it is theoretical, since the guided ligand immobilization allows the target analytes to be targeted to the region with a high field intensity, target molecules, especially those with a very low concentration, can produce an appreciable resonance shift in real LSPR sensing applications.

Although NSL is one of the most widely used techniques due to large-scale nanopatterned arrays and simple fabrication process, its inherent limitations such as the defective formation of nanosphere arrays and the limited pattern design make NIL more appropriate for marketable LSPR biosensor. As mentioned above, NIL is a stamp-based, low-cost, and high-throughput lithographic method that can generate largely patterned areas with sub-10 nm resolution. As an example of combining the NIL with a LSPR biosensor, Lee *et al.* described the fabrication of elliptical Au nanodisk arrays as a LSPR sensing substrate for clinical immunoassay via thermal NIL and showed an enhancement in the sensitivity of the detection of the prostate-specific antigen using the precipitation of 5-bromo-4-chloro-3-indolyl phosphate p-toluidine/nitro blue tetrazolium, catalyzed by alkaline phosphatase [59]. As presented in Fig. 7, gold nanodisks

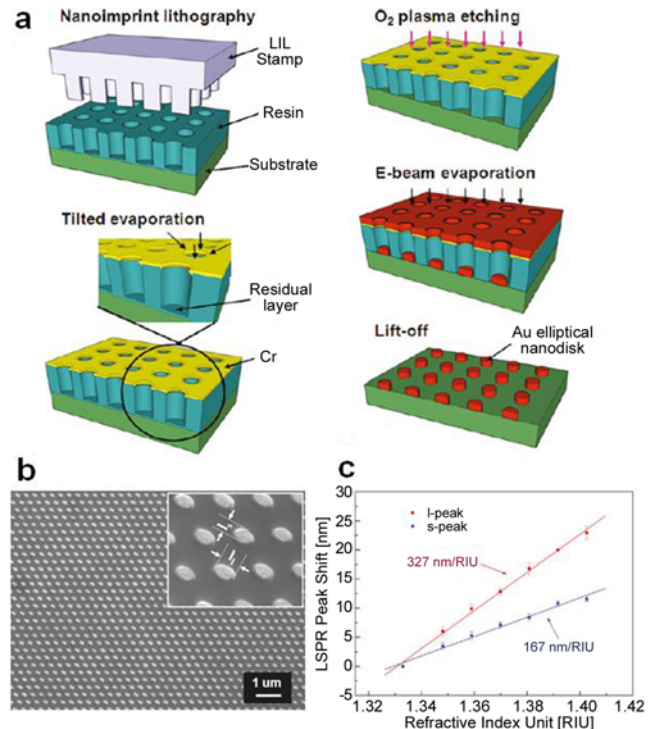


**Fig. 7.** (a) Fabrication of Au nanodisk arrays using nanoimprint lithography. Imprinting the elliptical Au nanodisk arrays, depositing the mask layer of Cr by tilted evaporation to create an undercut, removing the residual layer by  $\text{O}_2$  plasma etching, evaporating 1 nm Ti/20 nm Au film, and lifting off the imprint resin are performed sequentially. (b) SEM images of the array pattern of elliptical Au nanodisks fabricated on a glass wafer and (c) sensitivity characteristics to the bulk refractive index for the two different LSPR peaks of the prepared elliptical Au nanodisk arrays, measured in the transmission mode. (Reprinted with permission from [59]. Copyright 2011 American Chemical Society.)

were fabricated on glass through an unconventional tilted evaporation, which could preserve the thickness of imprinted resists and create an undercut beneficial to the subsequent lift-off process without any damage to pattern dimension and the glass while removing the residual polymers. In terms of the sensor performance, the sensitivity to the bulk refractive index was measured as 327 and 167 nm/RIU for the two different wavelength peaks, respectively. This large change in local refractive index because of the precipitation on the Au nanodisks amplified the wavelength shift of the LSPR peak, resulting in femtomolar detection limits, which was  $\sim 105$ -fold lower than the label-free detection without the enzyme precipitation.

## CONCLUSION

In this review, we explored a variety of fabrication methods that the performance and possible applications of the plasmonic nanostructures depend greatly on. It is thus important to

develop a fast, robust, low-cost, and mass production compatible technique of producing plasmonic substrate of a nanoscale feature size. In particular, rapidly evolving fabrication techniques of plasmonic nanostructures offer several research opportunities including plasmonic light source, photovoltaic devices, and high-sensitivity LSPR biosensor systems. While not presented here, ultra-low-loss optical interconnects, plasmonic waveguides, plasmonic nanolithography, imaging below the diffraction limit, and materials with a negative refractive index are another interesting areas that fascinate a large number of researchers [60].

These plasmonic studies based on nanoscale plasmonic structures provide an exciting and promising alternative to surmount the limitations of conventional optical systems with micrometer-scale bulky components. Hence, the manipulation of optical properties by adjusting the geometric parameters of the nanostructured substrates is currently the hot issue in the area of nanoscale plasmonics. Especially, it should be emphasized that, in order to achieve a breakthrough for a full realization of the potential applications of plasmon-based photonics, a greater collaboration in a variety of fields is very much required. Together with a better understanding of the underlying fundamentals and a development of theoretical analysis algorithms, advances in the areas of such as nanofabrication and integrated optics for miniaturization are all essential for the fulfillment of the promise by plasmonics. Relevant in-depth studies are currently under way in many research groups and in the near future, it is hoped that nanoscale optical system with a greater performance will be in widespread use, satisfying the various needs of the consumers.

## ACKNOWLEDGMENTS

This work was supported of Korea Science and Engineering Foundation (KOSEF) grant funded by the Korean government (MEST) (2011-0005517).

## REFERENCES

- [1] Homola J, Yee SS, Gauglitz G. Surface plasmon resonance sensors. *Sensor Actuat B-Chem*. 1999; 54(1-2):3-15.
- [2] Gao H, Henzie J, Odom TW. Direct evidence for surface plasmon-mediated enhanced light transmission through metallic nanohole arrays. *Nano Lett*. 2006; 6(9):2104-8.
- [3] Lamprecht B, Krenn JR, Schider G, Ditlbacher H, Salerno M, Felidj N, Leitner A, Aussenegg FR. Surface plasmon propagation in microscale metal stripes. *Appl Phys Lett*. 2001; 79(1):51-3.
- [4] Lal S, Link S, Halas NJ. Nano-optics from sensing to waveguiding. *Nat Photon*. 2007; 1:641-8.
- [5] Ozbay E. Plasmonics: merging photonics and electronics at nanoscale dimensions. *Science*. 2006; 311(5758):189-93.
- [6] Hutter E, Fendler JH. Exploitation of localized surface plasmon resonance. *Adv Mater*. 2004; 16(19):1685-706.
- [7] Daniel MC, Astruc D. Gold nanoparticles: assembly, supramolecular chemistry, quantum-size-related properties, and applications toward biology, catalysis, and nanotechnology. *Chem Rev*. 2004; 104(1):293-346.
- [8] Xia Y, Halas NJ. Shape-controlled synthesis and surface plasmonic properties of metallic nanostructures. *MRS Bull*. 2005; 30(5), 338-48.
- [9] Haes AJ, Haynes CL, McFarland AD, Schatz GC, Van Duyne RP, Zou S. Plasmonic materials for surface-enhanced sensing and spectroscopy. *MRS Bull*. 2005; 30(5), 368-75.
- [10] Whitney AV, Elam JW, Zou S, Zinovev AV, Stair PC, Schatz GC, Van Duyne RP. Localized surface plasmon resonance nanosensor: a high-resolution distance-dependence study using atomic layer deposition. *J Phys Chem B*. 2005; 109(43):20522-8.
- [11] Barnes WL. Surface plasmon-polariton length scales: a route to sub-wavelength optics. *J Opt A: Pure Appl Opt*. 2006; 8(4):S87-93.
- [12] Barnes WL. Fluorescence near interfaces: the role of photonic mode density. *J Mod Optic*. 1998; 45(4):661-99.
- [13] Hoa XD, Kirk AG, Tabrizian M. Towards integrated and sensitive surface plasmon resonance biosensors: a review of recent progress. *Biosens Bioelectron*. 2007; 23(2):151-60.
- [14] Prodan E, Radloff C, Halas NJ, Nordlander P. A hybridization model for the plasmon response of complex nanostructures. *Science*. 2003; 302(5644):419-22.
- [15] Shalaev VM, Botet R, Jullien R. Resonant light scattering by fractal clusters. *Phys Rev B*. 1991; 44(22):12216-25.
- [16] Nie S, Emory SR. Probing single molecules and single nanoparticles by surface-enhanced Raman scattering. *Science*. 1997; 275(5303):1102-6.
- [17] Wang S, Pile DFP, Sun C, Zhang X. Nanopin plasmonic resonator array and its optical properties. *Nano Lett*. 2007; 7(4):1076-80.
- [18] Khoury M, Ferry DK. Effect of molecular weight on poly(methyl methacrylate) resolution. *J Vac Sci Technol B*. 1996; 14(1):75-9.
- [19] Tseng AA, Chen K, Chen CD, Ma KJ. Electron beam lithography in nanoscale fabrication: recent development. *IEEE T Electr Pack*. 2003; 26(2):141-9.
- [20] Barbillion G, Bijeon JL, Plain J, de la Chapelle ML, Adam PM, Royer P. Electron beam lithography designed chemical nanosensors based on localized surface plasmon resonance. *Surf Sci*. 2007; 601(21):5057-61.
- [21] Hoa XD, Martin M, Jimenez A, Beauvais J, Charette P, Kirk A, Tabrizian M. Fabrication and characterization of patterned immobilization of quantum dots on metallic nano-gratings. *Biosens Bioelectron*. 2008; 24(4):970-5.
- [22] Cleary A, Clark A, Glidle A, Cooper JM, Cumming D. Fabrication of double split metallic nanorings for Raman sensing. *Microelectron Eng*. 2009; 86(4-6):1146-9.
- [23] Stodolka J, Nau D, Frommberger M, Zanke C, Giessen H, Quandt E. Fabrication of two-dimensional hybrid photonic crystals utilizing electron beam lithography. *Microelectron Eng*. 2005; 78-79:442-7.
- [24] Jin M, Pully V, Otto C, van den Berg A, Carlen ET. High-density periodic arrays of self-aligned subwavelength nanopillars for surface-enhanced Raman spectroscopy. *J Phys Chem C*. 2010; 114(50):21953-9.
- [25] Koh AL, Fernández-Domínguez AI, McComb DW, Maier SA, Yang JKW. High-resolution mapping of electron-beam-excited plasmon modes in lithographically defined gold nanostructures. *Nano Lett*. 2011; 11(3):1323-30.

- [26] Segawa H, Ueno K, Yokota Y, Misawa H, Yano T, Shibata S. Nano-patterning of a TiO<sub>2</sub>-organic hybrid material assisted by a localized surface plasmon. *J Am Ceram Soc.* 2010; 93(6):1634-8.
- [27] Murazawa N, Ueno K, Mizeikis V, Juodkakis S, Misawa H. Spatially selective nonlinear photopolymerization induced by the near-field of surface plasmons localized on rectangular gold nanorods. *J Phys Chem C.* 2009; 113(4):1147-9.
- [28] Ebbesen TW, Lezec HJ, Ghaemi HF, Thio T, Wolff PA. Extraordinary optical transmission through sub-wavelength hole arrays. *Nature.* 1998; 391:667-9.
- [29] Genet C, Ebbesen TW. Light in tiny holes. *Nature.* 2007; 445:39-46.
- [30] Barnes WL, Murray WA, Dintinger J, Devaux E, Ebbesen TW. Surface plasmon polaritons and their role in the enhanced transmission of light through periodic arrays of subwavelength holes in a metal film. *Phys Rev Lett.* 2004; 92(10):107401.
- [31] Gao H, Henzie J, Odom TW. Direct evidence for surface plasmon-mediated enhanced light transmission through metallic nanohole arrays. *Nano Lett.* 2006; 6(9):2104-8.
- [32] Watt F, Bettiol AA, Van Kan JA, Teo EJ, Breese MBH. Ion beam lithography and nanofabrication: a review. *Int J Nanosci.* 2005; 4(3):269-86.
- [33] Stewart ME, Anderton CR, Thompson LB, Maria J, Gray SK, Rogers JA, Nuzzo RG. Nanostructured plasmonic sensors. *Chem Rev.* 2008; 108(2):494-521.
- [34] Beermann J, Søndergaard T, Novikov SM, Bozhevolnyi SI, Devaux E, Ebbesen TW. Field enhancement and extraordinary optical transmission by tapered periodic slits in gold films. *New J Phys.* 2011; 13(6):063029.
- [35] Song Y, Elsayed-Ali HE. Aqueous phase Ag nanoparticles with controlled shapes fabricated by a modified nanosphere lithography and their optical properties. *Appl Surf Sci.* 2010; 256(20):5961-7.
- [36] Haynes CL, Van Duyne. Nanosphere lithography: a versatile nanofabrication tool for studies of size-dependent nanoparticle optics. *J Phys Chem B.* 2001; 105(24):5599-611.
- [37] Yonzon CR, Stuart DA, Zhang X, McFarland AD, Haynes CL, Van Duyne RP. Towards advanced chemical and biological nanosensors-an overview. *Talanta.* 2005; 67(3):438-48.
- [38] Lee FY, Fung KH, Tang TL, Tam WY, Chan CT. Fabrication of gold nano-particle arrays using two-dimensional templates from holographic lithography. *Curr Appl Phys.* 2009; 9(4):820-5.
- [39] Wang X, Xu J, Lee JCW, Pang YK, Tam WY, Chan CT, Sheng P. Realization of optical periodic quasicrystals using holographic lithography. *Appl Phys Lett.* 2006; 88(5):051901.
- [40] Schattenburg ML, Aucoin RJ, Fleming RC. Optically matched trilevel resist process for nanostructure fabrication. *J Vac Sci Technol B.* 1995; 13(6):3007-11.
- [41] Romanato F, Kang HK, Lee KH, Ruffato G, Prasciolu M, Wong CC. Interferential lithography of 1D thin metallic sinusoidal gratings: accurate control of the profile for azimuthal angular dependent plasmonic effects and applications. *Microelectron Eng.* 2009; 86(4-6):573-6.
- [42] Sahoo PK, Vogelsang K, Schiff H, Solak HH. Surface plasmon resonance in near-field coupled gold cylinder arrays fabricated by EUV-interference lithography and hot embossing. *Appl Surf Sci.* 2009; 256(2):431-4.
- [43] Boltasseva A. Plasmonic components fabrication via nanoimprint. *J Opt A: Pure Appl Opt.* 2009; 11(11):114001.
- [44] Hong SH, Bae BJ, Yang KY, Jeong JH, Kim HS, Lee H. Fabrication of sub-50 nm Au nanowires using thermally curing nanoimprint lithography. *Electron Mater Lett.* 2009; 5(4):139-43.
- [45] Fuchs A, Bender M, Plachetka U, Kock L, Koo N, Wahlbrink T, Kurz H. Lithography potentials of UV-nanoimprint. *Curr Appl Phys.* 2008; 8(6):669-74.
- [46] Guo LJ. Recent progress in nanoimprint technology and its applications. *J Phys D: Appl Phys.* 2004; 37(11):R123-41.
- [47] Okamoto K, Niki I, Shvartsner A, Narukawa Y, Mukai T, Scherer A. Surface-plasmon-enhanced light emitters based on InGaN quantum wells. *Nat Mater.* 2004; 3:601-5.
- [48] Okamoto K, Niki I, Scherer A, Narukawa Y, Mukai T, Kawakami Y. Surface plasmon enhanced spontaneous emission rate of InGaN/GaN quantum wells probed by time-resolved photoluminescence spectroscopy. *Appl Phys Lett.* 2005; 87(7):071102.
- [49] Reboud V, Kehagias N, Zelsmann M, Schuster C, Fink M, Reuther F, Gruetzner G, Torres CMS. Photoluminescence enhancement in nanoimprinted photonic crystals and coupled surface plasmons. *Opt Express.* 2007; 15(12):7190-5.
- [50] Gwon M, Lee E, Kim DW, Yee KJ, Lee MJ, Kim YS. Surface-plasmon-enhanced visible-light emission of ZnO/Ag grating structures. *Opt Express.* 2011; 19(7):5895-901.
- [51] Catchpole KR, Polman A. Plasmonic solar cells. *Opt Express.* 2008; 16(26):21793-800.
- [52] Atwater HA, Polman A. Plasmonics for improved photovoltaic devices. *Nat Mater.* 2010; 9:205-13.
- [53] Kang MG, Xu T, Park HJ, Luo X, Guo LJ. Efficiency enhancement of organic solar cells using transparent plasmonic Ag nanowire electrodes. *Adv Mater.* 2010; 22(39):4378-83.
- [54] Zhao J, Zhang X, Yonzon CR, Haes AJ, Van Duyne RP. Localized surface plasmon resonance biosensors. *Nanomedicine.* 2006; 1(2):219-28.
- [55] Byun KM. Development of nanostructured plasmonic substrates for enhanced optical biosensing. *J Opt Soc Korea.* 2010; 14(2):65-76.
- [56] Byun KM, Jang SM, Kim SJ, Kim D. Effect of target localization on the sensitivity of a localized surface plasmon resonance biosensor based on subwavelength nanostructures. *J Opt Soc Am A.* 2009; 26(4):1027-34.
- [57] Jang SM, Kim D, Choi SH, Byun KM, Kim SJ. Enhancement of localized surface plasmon resonance detection by incorporating metal-dielectric double-layered subwavelength gratings. *Appl Opt.* 2011; 50(18):2846-54.
- [58] Kim NH, Jung WK, Byun KM. Correlation analysis between plasmon field distribution and sensitivity enhancement in reflection- and transmission-type localized surface plasmon resonance biosensors. *Appl Opt.* 2011. (To be published)
- [59] Lee SW, Lee KS, Ahn J, Lee JJ, Kim MG, Shin YB. Highly sensitive biosensing using arrays of plasmonic Au nanodisks realized by nanoimprint lithography. *ACS Nano.* 2011; 5(2):897-904.
- [60] Murray WA, Barnes WL. Plasmonic materials. *Adv Mater.* 2007; 19(22):3771-82.